Available online at www.sciencedirect.com
ScienceDirect
Ceramics International 37 (2011) 1725–1729
CERAMICS INTERNATIONAL
www.elsevier.com/locate/ceramint

Effect of holmium on the magnetic and electrical properties of barium based W-type hexagonal ferrites

Faiza Aen [a], Shahida B. Niazi [b], M.U. Islam [a], Mukhtar Ahmad [a], M.U. Rana [a,*]

[a] Department of Physics, Bahauddin Zakariya University, Multan 60800, Pakistan
[b] Department of Chemistry, Bahauddin Zakariya University, Multan 60800, Pakistan

Received 30 April 2010; received in revised form 18 August 2010; accepted 4 October 2010
Available online 30 October 2010

Abstract

A series of $BaHo_xFe_{16-x}O_{27}$ ($x = 0.0, 0.2, 0.4, 0.6, 0.8, 1.0$) W-type hexagonal ferrites were prepared by co-precipitation technique at high annealing temperature of 1320 °C. XRD reveals single W-type hexagonal phase in these ferrites. The grain size is measured by SEM analysis using line intercept method. Saturation magnetization, retentivity and coercivity were measured from MH-loops taken on VSM. It was observed that magnetization increases with the increase of Ho content due to difference in ionic radii of Ho^{3+} (0.901 Å) and Fe^{3+} (0.67 Å) ions. Room temperature dc resistivity increases as a function of Ho^{3+} that may be due to separation between grains. The dc electrical resistivity decreases as a function of temperature which indicates the semi-conducting behavior of the samples.

Keywords: W-type hexa ferrites; Rare earth substitution; X-ray diffraction; SEM analysis; Vibrating sample magnetometry; Resistivity

1. Introduction

Hexa ferrites prepared by wet method exhibit unique electrical and magnetic properties. These ferrites are also important due to their industrial applications having high coercivity and moderate saturation magnetization with large BH-energy product [1,2]. W-type hexa ferrites of $BaZn_2Cr_xFe_{16-x}O_{27}$ ($x \leq 1$) prepared by co-precipitation have been reported by Javed and Ali Khan [3]. Homogenous single phase nano-particles of Cr substituted powder were obtained. The lattice constants 'a' and 'c' of the chromium doped and undoped sample remain unchanged on increasing the substitution level of Cr. The room temperature resistivity of the doped sample was found to increases with the addition of chromium, because the Cr^{+3} ions act as scattering centers. Sharma et al. [4] studied the structural and magnetic properties of barium hexa ferrites $BaFe_{12-x}Mn_xO_{19}$. It was observed that the Ba-substitution did not affect the lattice parameters but produced smaller crystallites. The lower magnetization and higher coercivity was attributed to the reduction of average magnetic moment of the lattice and to the improvement in the crystallite size. Rare earth substituted $SrFe_{1-x}R_xO_{19}$ (R = La, Gd and Er; $x = 0.0, 0.5, 1.0$) ferrites studied by Rezlescu was reported [5]. The X-ray diffraction analysis revealed M-type hexagonal structure and magnetic properties were reported to be dependent on heat treatment conditions at 1000 °C. The heat treatment determined a reduced grain growth due to internal stress generated by 'R' ions. The coercivity increased after critical heat treatment time.

Polycrystalline ferrites $Sr_{0.5}Pb_{0.5}{}^{2+}Fe_{12-x}Pb_x{}^{3+}O_{19}$ were studied by Shahid and Asghari [6]. It was observed that the lattice parameters ('a' and 'c') increased with the increase in Pb content, which enhanced the X-ray density and porosity. DC electrical resistivity and activation energy were increased and mobility decreased by the substitution of Pb ions at room temperature on the basis of Verwey hopping model. $Zn_{2-x}Cu_xBaFe_{16}O_{27}$ Polycrystalline ferrites were prepared by ceramic method reported by Hemeda and Hemeda [7]. X-ray analysis confirmed the presence of W-type hexa ferrite phase at room temperature. It was observed that all hysteresis loops are closed which indicates low anisotropy field and low saturation magnetization field. The thermoelectric power decreased by increasing Cu^{2+} content due to hopping of holes between $Cu^{2+} \leftrightarrow Cu^{1+}$and the increase of electrical conductivity was

* Corresponding author. Tel.: +92 619210199; fax: +92 619210068.
E-mail address: mzharrana@bzu.edu.pk (M.U. Rana).

0272-8842/$36.00 © 2011 Published by Elsevier Ltd and Techna Group S.r.l.
doi:10.1016/j.ceramint.2010.10.006

mainly due to the increase of drift mobility with the increase of temperature. Choi et al. [8] studied (La–Co) substituted Sr based M-type hexa-ferrites, $(La–Co)_xSr_{1-x}Fe_{12-x}O_{19}$ powders synthesized by sol–gel process. The ferrite powders were sintered at 950 °C. Single phase M-type hexa ferrites were characterized by X-ray diffraction. It was observed that magnetization is 63.9 emu/g and coercivity increased with the increase of (La–Co) concentration. Attia et al. [9] reported the transport properties of W-type hexa ferrites with composition $BaZn_{2-x}Mg_xFe_{16}O_{27}$ and reported the dc and ac electrical conductivity. DC conductivity exhibits the existence of a transition temperature Ts, which is much lower than their Curie points. The results of AC conductivity revealed that the multiple hopping conduction mechanism might be predominant mechanism for these ferrites.

In the present work Ho-substituted W-type hexa ferrites have been prepared by co-precipitation and the effect of Ho-contents on the coercivity and electrical conductivity have been studied systematically.

2. Experimental

$BaHo_xFe_{16-x}O_{27}$ (x = 0.0, 0.2, 0.4, 0.8, 1.0) were prepared by co-precipitation technique. Analytical grade ferric chloride ($FeCl_3{\cdot}6H_2O$), barium nitrate ($Ba(NO_3)_2$), Zinc oxide(ZnO) and Holmium oxide (Ho_2O_3) were used as starting materials for the preparation of $BaHo_xFe_{16-x}O_{27}$ powder. After stoichiometric calculations the required amount of parent materials were isolated in de-ionized water. Since Ho_2O_3 is insoluble in water, first it was dissolved in nitric acid at 80 °C in order to convert it into nitrate and then poured into the prepared solution. Proportionate amount of NaOH and Na_2CO_3 was used as reagent to precipitate the metals as hydroxides. Calculated amount of NaOH and Na_2CO_3 were dissolved in 100 ml distilled water and added slowly drop-wise into metal solution with constant stirring until precipitation was complete. The precipitates were allowed to settle down and the supernatant liquid was tested with NaOH and Na_2CO_3 solution for any more precipitation. Filtration of precipitates was carried out with the help of filtration flask operating on a water suction pump.

The precipitates were thoroughly washed with distilled water until free from Cl^- ions, which were checked with $AgNO_3$ test. The precipitated product contained hydroxides of Ho^{3+}, Ba^{2+}, and Fe^{3+}. The product was dried in an electric oven at a temperature of 110 °C for 24h. The dried powder was mixed homogenously in an agate mortar and pestle for 2 h. Before and after this process, the mortar and pestle was rinsed with acetone. The dried powder was calcined at 1050 °C for 2 h, before final sintering and then pressed into pellets under the pressure of (∼35 KN/mm^2) using Paul-Otto Weber hydraulic press. The pellets were then finally sintered at 1320 °C for 8 h followed by air quenching. In the present work, the density was measured using Archimedes's principle. The bulk density was measured by using the relation;

$$D = \left[\frac{W_{air}}{W_{air} - W_{liquid}}\right] \times \text{density of toluene} \quad (1)$$

where W_{air} = weight of sample in air, W_{liquid} = weight of sample in liquid and density of toluene is 0.857 g/cm^3 where $W_{air} - W$-liquid = weight loss in liquid.

X-ray diffraction analysis was carried out using shimadzu X-ray diffractometer equipped with CuKα radiation (λ = 1.5406 Å) in order to confirm the phase developed. The MH loops were plotted using vibrating sample magnetometer (VSM) at room temperature. DC resistivity was measured by two probe method using source meter model 2400 (Keithley).

3. Results and discussion

3.1. Physical and structural properties

X-ray diffraction patterns show single phase W-type structure of all compositions as shown in the Fig. 1. The lattice parameters 'a' and 'c' were calculated by ab-inito method using following equation;

$$\text{Sin}^2\theta = \frac{\lambda^2}{3a^2}(h^2+hk+k^2) + \left(\frac{\lambda^2}{4c^2}\right)l^2 \quad (2)$$

The (c/a) ratio varies from 5.5 to 5.8, that falls in the allowed range of w type hexagonal ferrites.

The change in the values of 'a' and 'c' suggests that the Fe^{3+} ions have been substituted by RE^{3+} ions and this change is occurred due to difference between ionic radii of RE^{3+} and Fe^{3+} ions and interaction between rare earth and surrounding ions [10]. The ionic radius of Ho (0.901 Å) is greater which prefers octahedral sites followed by the migration of some Fe^{3+} (0.67 Å) ions from octahedral sites to tetrahedral sites [3,11]. Therefore with the increasing Ho content both lattice parameters 'a' and 'c' increases [12,13]. The variation of lattice parameters and the (c/a) ratio versus Ho concentration is given in Table 1. X-ray and bulk densities are also listed in Table 1.

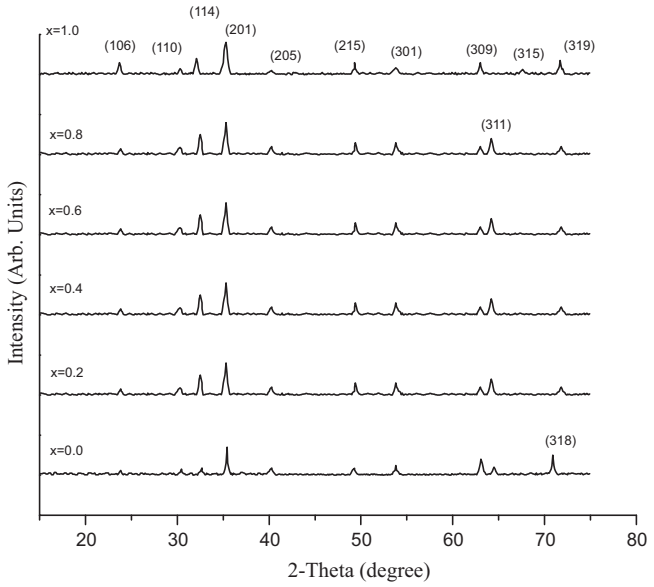

Fig. 1. X-ray diffraction patterns of $BaHo_xFe_{16-x}O_{27}$ ferrites (x = 0.0, 0.2, 0.4, 0.6, 0.8, 1.0).

Table 1
Lattice constants, *c/a* ratio, X-ray density, activation energy, resistivity of $BaHo_xFe_{16-x}O_{27}$ ferrites.

Parameters	$X = 0.0$	$X = 0.2$	$X = 0.4$	$X = 0.6$	$X = 0.8$	$X = 1.0$
Lattice constant a (Å)	5.86	5.87	5.88	5.87	5.88	5.91
Lattice constant c (Å)	32.6	32.87	33.34	33.30	33.5	33.45
c/a	5.55	5.59	5.67	5.67	5.69	5.66
X-ray density D_x (g cm^{-3})	5.01	5.03	5.07	5.11	5.13	5.16
Activation energy (eV)	0.178	0.413	0.619	1.23	0.55	0.318
Resistivity (((-cm at 298 K)	7.36×10^2	3.46×10^4	2.62×10^7	6.05×10^8	1.11×10^9	3.7×10^9

The X-ray density is defined as the actual density and was calculated by using the formula [6]:

$$D_x = \frac{2M}{N_A V} \tag{3}$$

'M' is the molar mass 'N_A' is Avogadro's number and 'V' is the volume of unit cell which is calculated using the relation, $V = a^2 c \sin 120^\circ$. It was observed that the X-ray density (D_x) increases from 5.0 to 5.5 (g/cm^3). The increase in X-ray density may be due to the greater atomic mass of Ho^{+3} (164.93 a.m.u) than that of Fe^{3+} (55.85 a.m.u) [6].

Fig. 2 shows few representative SEM micrographs of the $BaHo_xFe_{16-x}O_{27}$ hexagonal ferrites. The grain size measured from SEM micrographs varies from 205 to 188 nm respectively for the compositions $x = 0.0$, 0.2, 0.8.

3.2. Magnetic properties

The magnetic properties of all given samples have been investigated from MH-Loops and few are shown in Fig. 3. The saturation magnetization (M_s), remanance (M_r) and coercivity (H_c) are listed in Table 2. Saturation magnetization (M_s) and remanance (M_r) depend on the R^{3+} substitution for Fe^{3+} ions. Coercivity is a collective property of the system of interacting grains. In the present work our results show that the magnetization increases with the increase of Ho concentration because of larger magnetic moment of Ho (10 μ_B) than Fe (5 μ_B). The coercivity (H_c) increases that may be due to the enhancement of magneto crystalline anisotropy [14] with anisotropic Fe^{2+} ions located on 2A sites as usually found in rare earth substitution [15,16] and this happens due to elevated sintering temperature [17]. The

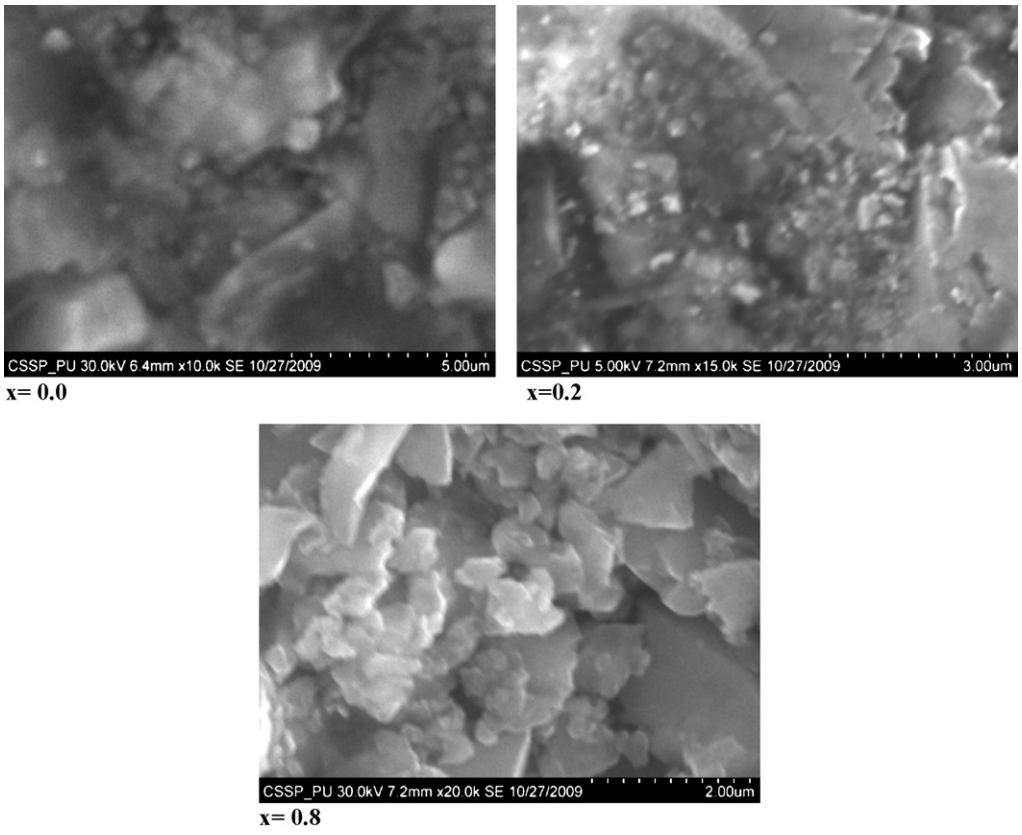

Fig. 2. SEM micrographs of the $BaHo_xFe_{16-x}O_{27}$ ferrites at $x = 0.0$, 0.2, 0.8.

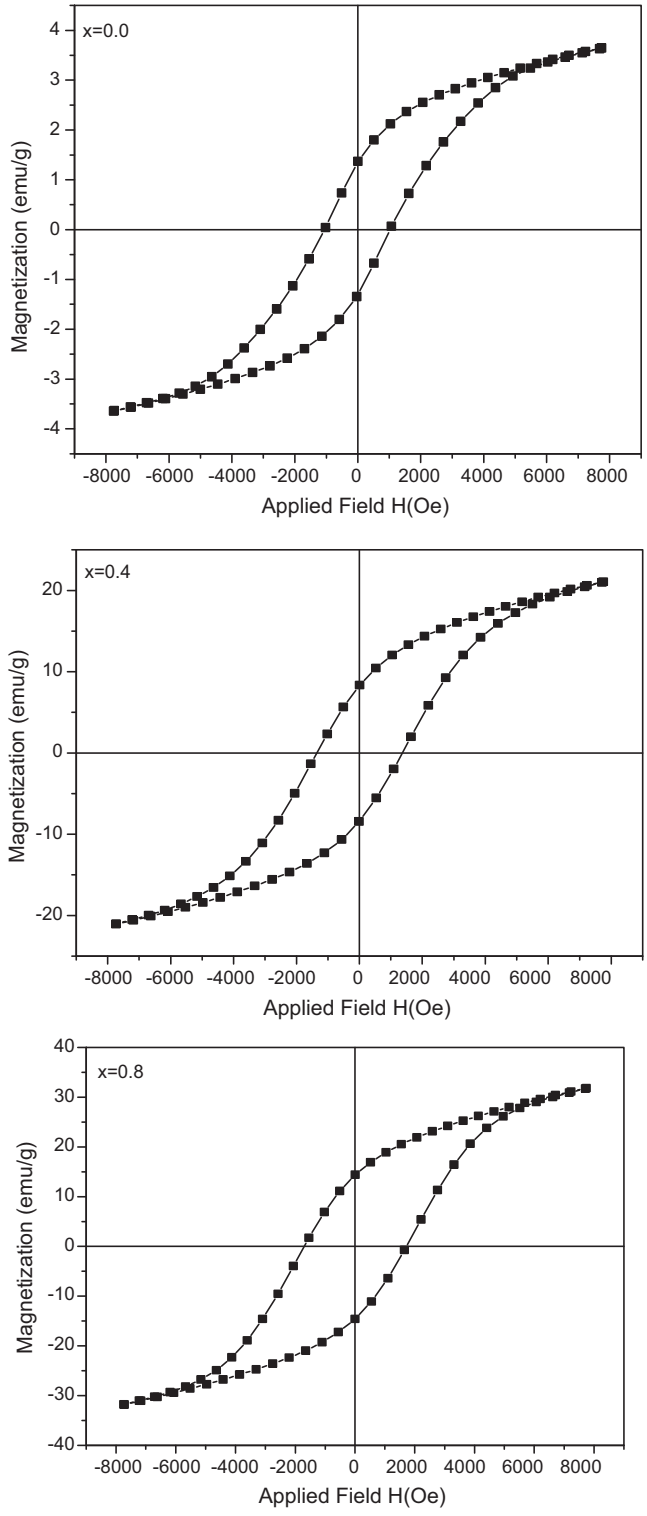

Fig. 3. . MH loops of few representative $BaHo_xFe_{16-x}O_{27}$ ferrites (x = 0.0, 0.4, 0.8).

coercivity increase with the increase of Ho concentration. It is observed that H_c is inversely proportional to the packing of magnetic materials or the grain size that is H_c α 1/r. Our results agree with the reported results on W-type hexagonal ferrites [18].

Table 2
Coercivity, saturation magnetization and remanance of $BaHo_xFe_{16-x}O_{27}$ ferrites.

Ho contents (x)	H_c (Oe)	M_s (emu/g)	M_r (emu/g)
0.0	1041.7	3.648	1.334
0.4	1358.4	21.078	8.347
0.8	1709.6	31.831	14.492

3.3. Electrical properties

Room temperature resistivity of $BaHo_xFe_{16-x}O_{27}$ ferrites was measured in the temperature range 40–200 °C is listed in Table 1. The room temperature resistivity increases significantly from 7.36×10^2 to 3.7×10^9 Ω-cm with the increase of Ho concentration. The room temperature resistivities of W-type hexa ferrites reported by various authors are found to be in the range of 10^4–10^7 Ω-cm [13,3]. Our results of resistivity fall in the reported range. The increase in the resisitivity may be attributed to the obstruction in the Verwey mechanism due to larger density of grain boundaries produced by fine grains. Moreover the resistivity of Ho (81.4×10^{-8} Ω-m) is larger than Fe (9.71×10^{-8} Ω-m) and Ba (33.2×10^{-8} Ω-m) at 300 K which is responsible for the enhancement of resistivity.

Temperature dependent dc electrical resistivity is shown in the Fig. 4. It can be seen that as the temperature increases the resistivity decreases verifying the equation:

$$\rho = \rho_o \exp\left(\frac{E_a}{k_B T}\right) \quad (4)$$

where k_B is the Boltzmann's constant and T is absolute temperature. It also showed that by increasing temperature, the conductivity of ferrite increases, indicating that these ferrites exhibit semiconducting behavior. The activation energy (E_a) of hopping for the different samples was calculated Arrhenius

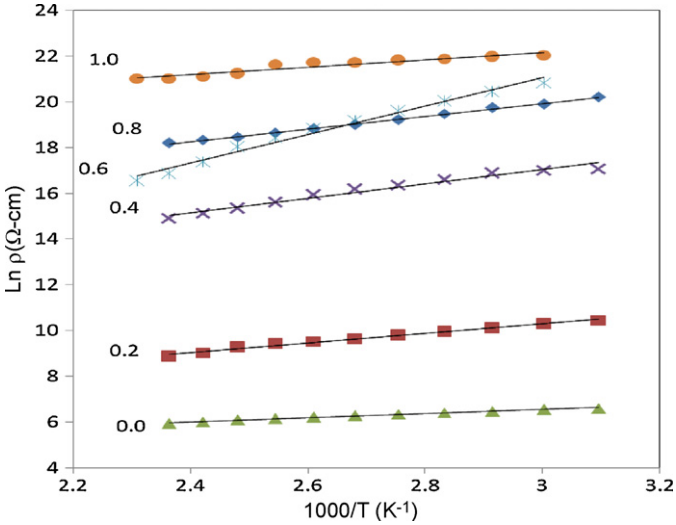

Fig. 4. Arrhenius plots of $BaHo_xFe_{16-x}O_{27}$ ferrites (x = 0.0, 0.2, 0.4, 0.6, 0.8, 1.0).

plots. The increase in activation energy may be attributed to the creation of more cations and developing of oxygen vacancies which might have been produced due to rise in temperature. It is concluded that concentration of oxygen vacancies is an important factor in sintering process as well as in DC electrical resistivity [6].

4. Conclusions

The co-precipitation method is found suitable for preparation of homogenous single phase nano-particle of Ho doped hexa ferrites. The lattice constants 'a' and 'c' increased with the increase of Ho concentration due to large ionic radius of Ho. Coercivity follows $H_c \ \alpha \ 1/r$ behavior. DC electrical resistivity increases due to large density of grain boundaries that hinder the Verway mechanism. The present samples are useful at high frequency applications due to enhanced resistivity and coercivity. The last two sample ($x = 0.8$ and 1.0) have highest resistivity which are the best samples in the present studies.

Acknowledgements

Dr. Pietro Vincenzini General Editor–Ceramics International P.O. Box 174-Corso Mazzini No. 52 48018 Faenza, Italy.

References

[1] R.H. Vidora, J. Appl. Phys. 63 (1988) 3423.
[2] A. Atare, I.R. Harris, C.B. Ponton, J. Mater. Sci. 30 (1995) 1429.
[3] M. Javed Iqbal, Ali Khan F. R., J. Alloys Compd. 478 (2009) 847–852.
[4] P. Sharma, R.A. Rocha, S.N. Medeiros, B. Halloouche, A. Paesano Jr., J. Magn. Magn. Mater. 316 (2007) 29–33.
[5] N. Rezlescu, C. Doroftei, E. Rezlescu, P.D. Popa, J. Alloys Compd. 451 (2008) 492–496.
[6] H. Shahid, M. Asghari, J. Alloys Compd. 466 (2008) 293–298.
[7] D.M. Hemeda, O.M. Hemeda, J. Magn. Magn. Mater. 320 (2008) 1557–1562.
[8] D.H. Choi, S.w. Zee, I.-B. Shim, C.S. Kim, J. Magn. Magn. Mater. 304 (2006) e243–e245.
[9] S.M. Attia, A.M. Abo El Atab, D. El Konyb, J. Magn. Magn. Mater. 270 (2004) 142–151.
[10] Wang Jing, Zhang Hong, Bai Shuxin, Chen Ke, Zhang Changrui, J. Magn. Magn. Mater. 312 (2007) 310–313.
[11] J.F. Wang, C.B. Proton, I.R. Harris, J. Alloys Compd. 104 (2005) 403.
[12] M.A. Ahmed, N. Okasha, M. Oaf, R.M. Kershi, J. Magn. Magn. Mater. 314 (2007) 128–134.
[13] A.M. Abo El Ata, F.M. Reicha, M.M. Ali, J. Magn. Magn. Mater. 292 (2005) 17–24.
[14] S. Ounnunkad, J. Solid State Commun. 138 (2006) 472–475.
[15] A.M. Van Diepan, F.K. Lotgering, J. Phys. Chem. Solids 35 (1974) 1641.
[16] Ch. Sauer, U. Kobler, W. Zinn, H. Stablein, J. Phys. Chem. Solids 39 (1978) 1197.
[17] Xiao-Hui Wang, Tian-Ling Ren, Long-Yuli, Lian-Sheng Zhang, J. Magn. Magn. Mater. 184 (1998) 95–100.
[18] D.M. Hemeda, A. Al-Sharif, O.M. Hemeda, J. Magn. Magn. Mater. 315 (2007) L1–L7.